Closed-form Green's Functions for Stratified Uniaxial Anisotropic Medium

P. P. Ding[1,2], S. Zouhdi[1], L. W. Li[2], and S. P. Yeo[2]

[1]Laboratoire de Genie Electrique de Paris, Supelec, France
[2]Department of Electrical and Computer Engineering, National University of Singapore, Singapore

Abstract— The spatial-domain Green's functions for electric and magnetic fields are cast into closed forms with two-level approximation of the spectral-domain Green's functions in the stratified uniaxial anisotropic medium. The spectral-domain Green's functions for general source and observation points are derived by the wave iterative algorithm. The explicit formulations reduced to the isotropic case agrees well with the existing results corresponding to the isotropic medium. By using the discrete complex image method, the closed-form Green's functions are obtained in the spatial domain. Numerical examples show that the closed-form Green's functions in the stratified uniaxial anisotropic medium have good accuracy and efficiency.

1. INTRODUCTION

The dyadic Green's function in the stratified uniaxial anisotropic medium has attracted much attention because of its wide range of practical applications, ranging from geophysics to microwave integrated circuits [1–4]. For the last decades, several methods have been employed for the derivation of the spectral-domain Green's functions in the stratified uniaxial anisotropic medium, including wave iterative technique [5] and cylindrical vector eigenfunction expansion method [6]. The wave iterative technique uses the kDB system of coordinates and the Fourier transform to derive the unbounded Green's function formulation and then the dyadic Green's function in any arbitrary layer is obtained in terms of the global upward and downward reflection and transmission matrices. The cylindrical vector eigenfunction expansion technique uses the Ohm-Rayleigh method and a set of solenoidal vector wave functions to derive the unbounded Green's function and then the general scattering dyadic Green's function in any arbitrary layer is obtained by using the scattering superposition. Due to the sufficiently complicated formulations in terms of the defined dyadic or matrix, the closed-form Green's functions in the spatial domain are quite difficult to obtain by the two methods.

It is the purpose of this paper to present a complete set of formulations for the dyadic Green's function in the stratified uniaxial anisotropic medium and to calculate the closed-form Green's functions in the spatial domain. The electromagnetic fields are obtained in terms of dyadic Green's functions of electric or magnetic type represented in the spatial domain. Section 2 deals with the formulations of the dyadic Green's functions for arbitrary locations of the source and observation point. By using the discrete complex image method (DCIM), the closed-form Green's function can be successfully obtained [7]. In Section 3, in order to verify the accuracy of the present formulations, they are compared with existing results corresponding to isotropic medium which have been well-documented [8, 9]. Then, several numerical results are presented to show the efficiency and accuracy of the closed-form Green's function, compared with the exact Green's function obtained by the numerical integration.

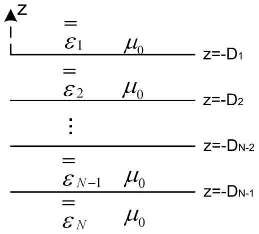

Figure 1: Geometry of the stratied uniaxial anisotropic medium.

2. FORMULATION

For the sake of illustration, we consider a stratified uniaxial anisotropic medium with optic axis in the $\hat{z}$ direction, as shown in Fig. 1. The wave iterative method presented in [5] is employed to construct the dyadic Green's functions in the spectral domain. In the presence of an arbitrary oriented electric current point source, the Green's functions can be represented as (1), (8), (13), corresponding to the relatively different locations between the source point and the observation point. The source and observation point is located at the layer m and n, respectively. The formulations related with the magnetic field Green's functions and the magnetic sources have the similar forms, which are not detailed here. The fields are assumed to vary harmonically as $e^{-i\omega t}$ in this work.

When $m = n$,

$$\begin{aligned}
\overline{\overline{G}}_{nn}(\mathbf{r},\mathbf{r}') =& \frac{1}{i\omega\hat{z}\cdot\overline{\overline{\varepsilon}}_n\cdot\hat{z}}\hat{z}\hat{z}\delta(\mathbf{r}-\mathbf{r}') - \frac{\omega\mu_n}{4\pi}\int_0^\infty dk_\rho\, k_\rho\cdot J_0(k_\rho\rho)\cdot\Big[e^{i\gamma_{\mathrm{I}\alpha}^{(n)}(z_n-z_n')}\mathbf{e}_{\mathrm{I}\alpha}^{(n)}\mathbf{u}_{\mathrm{I}\alpha}^{(n)} \\
&+e^{i\gamma_{\mathrm{II}\alpha}^{(n)}(z_n-z_n')}\mathbf{e}_{\mathrm{II}\alpha}^{(n)}\mathbf{u}_{\mathrm{II}\alpha}^{(n)} + e^{i\gamma_{\mathrm{I}u}^{(n)}(z_n-z_n')}A_1^{(1,1)}\mathbf{e}_{\mathrm{I}u}^{(n)}\mathbf{u}_{\mathrm{I}u}^{(n)} + e^{i\gamma_{\mathrm{I}u}^{(n)}z_n-i\gamma_{\mathrm{II}u}^{(n)}z_n'}A_1^{(1,2)}\mathbf{e}_{\mathrm{I}u}^{(n)}\mathbf{u}_{\mathrm{II}u}^{(n)} \\
&+e^{i\gamma_{\mathrm{II}u}^{(n)}z_n-i\gamma_{\mathrm{I}u}^{(n)}z_n'}A_1^{(2,1)}\mathbf{e}_{\mathrm{II}u}^{(n)}\mathbf{u}_{\mathrm{I}u}^{(n)} + e^{i\gamma_{\mathrm{II}u}^{(n)}(z_n-z_n')}A_1^{(2,2)}\mathbf{e}_{\mathrm{II}u}^{(n)}\mathbf{u}_{\mathrm{II}u}^{(n)} + e^{i\gamma_{\mathrm{I}u}^{(n)}z_n-i\gamma_{\mathrm{I}d}^{(n)}z_n'}A_2^{(1,1)}\mathbf{e}_{\mathrm{I}u}^{(n)}\mathbf{u}_{\mathrm{I}d}^{(n)} \\
&+e^{i\gamma_{\mathrm{I}u}^{(n)}z_n-i\gamma_{\mathrm{II}d}^{(n)}z_n'}A_2^{(1,2)}\mathbf{e}_{\mathrm{I}u}^{(n)}\mathbf{u}_{\mathrm{II}d}^{(n)} + e^{i\gamma_{\mathrm{II}u}^{(n)}z_n-i\gamma_{\mathrm{I}d}^{(n)}z_n'}A_2^{(2,1)}\mathbf{e}_{\mathrm{II}u}^{(n)}\mathbf{u}_{\mathrm{I}d}^{(n)} + e^{i\gamma_{\mathrm{II}u}^{(n)}z_n-i\gamma_{\mathrm{II}d}^{(n)}z_n'}A_2^{(2,2)}\mathbf{e}_{\mathrm{II}u}^{(n)}\mathbf{u}_{\mathrm{II}d}^{(n)} \\
&+e^{i\gamma_{\mathrm{I}d}^{(n)}z_n-i\gamma_{\mathrm{I}u}^{(n)}z_n'}A_3^{(1,1)}\mathbf{e}_{\mathrm{I}d}^{(n)}\mathbf{u}_{\mathrm{I}u}^{(n)} + e^{i\gamma_{\mathrm{I}d}^{(n)}z_n-i\gamma_{\mathrm{II}u}^{(n)}z_n'}A_3^{(1,2)}\mathbf{e}_{\mathrm{I}d}^{(n)}\mathbf{u}_{\mathrm{II}u}^{(n)} + e^{i\gamma_{\mathrm{II}d}^{(n)}z_n-i\gamma_{\mathrm{I}u}^{(n)}z_n'}A_3^{(2,1)}\mathbf{e}_{\mathrm{II}d}^{(n)}\mathbf{u}_{\mathrm{I}u}^{(n)} \\
&+e^{i\gamma_{\mathrm{II}d}^{(n)}z_n-i\gamma_{\mathrm{II}u}^{(n)}z_n'}A_3^{(2,2)}\mathbf{e}_{\mathrm{II}d}^{(n)}\mathbf{u}_{\mathrm{II}u}^{(n)} + e^{i\gamma_{\mathrm{I}d}^{(n)}(z_n-z_n')}A_4^{(1,1)}\mathbf{e}_{\mathrm{I}d}^{(n)}\mathbf{u}_{\mathrm{I}d}^{(n)} + e^{i\gamma_{\mathrm{I}d}^{(n)}z_n-i\gamma_{\mathrm{II}d}^{(n)}z_n'}A_4^{(1,2)}\mathbf{e}_{\mathrm{I}d}^{(n)}\mathbf{u}_{\mathrm{II}d}^{(n)} \\
&+e^{i\gamma_{\mathrm{II}d}^{(n)}z_n-i\gamma_{\mathrm{I}d}^{(n)}z_n'}A_4^{(2,1)}\mathbf{e}_{\mathrm{II}d}^{(n)}\mathbf{u}_{\mathrm{I}d}^{(n)} + e^{i\gamma_{\mathrm{II}d}^{(n)}(z_n-z_n')}A_4^{(2,2)}\mathbf{e}_{\mathrm{II}d}^{(n)}\mathbf{u}_{\mathrm{II}d}^{(n)}\Big]
\end{aligned}\tag{1}$$

where

$$\mathbf{A}_2 = \left[\mathbf{G}_u^{(n)}(z_n=-D_n)\right]^{-1}\cdot\mathbf{R}_{Dn,n+1}\cdot\mathbf{N}_n\cdot\left[\mathbf{G}_d^{(n)}(z_n=-D_n)\right]\tag{2}$$

$$\mathbf{A}_1 = \mathbf{A}_2\cdot\mathbf{G}_d^{(n)}(z_n=D_{n-1})\cdot\mathbf{R}_{Un,n-1}\cdot\mathbf{G}_u^{(n)}(z_n=-D_{n-1})\tag{3}$$

$$\mathbf{A}_3 = \left[\mathbf{G}_d^{(n)}(z_n=-D_{n-1})\right]^{-1}\cdot\mathbf{R}_{Un,n-1}\cdot\mathbf{M}_n\cdot\left[\mathbf{G}_u^{(n)}(z_n=-D_{n-1})\right]\tag{4}$$

$$\mathbf{A}_4 = \mathbf{A}_3\cdot\mathbf{G}_u^{(n)}(z_n=D_n)\cdot\mathbf{R}_{Dn,n+1}\cdot\mathbf{G}_d^{(n)}(z_n=-D_n)\tag{5}$$

$$\mathbf{M}_n = \left[\mathbf{I}-\mathbf{G}_u^{(n)}(z_n=-D_{n-1}+D_n)\cdot\mathbf{R}_{Dn,n+1}\cdot\mathbf{G}_d^{(n)}(z_n=-D_n+D_{n-1})\cdot\mathbf{R}_{Un,n-1}\right]^{-1}\tag{6}$$

$$\mathbf{N}_n = \left[\mathbf{I}-\mathbf{G}_d^{(n)}(z_n=-D_n+D_{n-1})\cdot\mathbf{R}_{Un,n-1}\cdot\mathbf{G}_u^{(n)}(z_n=-D_{n-1}+D_n)\cdot\mathbf{R}_{Dn,n+1}\right]^{-1}\tag{7}$$

When the source point z' is located above the observation point z, α is equal to d. Otherwise, α is equal to u.

When $m > n$,

$$\begin{aligned}
\overline{\overline{G}}_{nm}(\mathbf{r},\mathbf{r}') =& -\frac{\omega\mu_m}{4\pi}\int_0^\infty dk_\rho\, k_\rho\cdot J_0(k_\rho\rho)\cdot\Big[e^{i\gamma_{\mathrm{I}u}^{(n)}(z_n+D_n)+i\gamma_{\mathrm{I}u}^{(m)}(-z_m'-D_{m-1})}B_1^{(1,1)}\mathbf{e}_{\mathrm{I}u}^{(n)}\mathbf{u}_{\mathrm{I}u}^{(m)} \\
&+e^{i\gamma_{\mathrm{I}u}^{(n)}(z_n+D_n)+i\gamma_{\mathrm{II}u}^{(m)}(-z_m'-D_{m-1})}B_1^{(1,2)}\mathbf{e}_{\mathrm{I}u}^{(n)}\mathbf{u}_{\mathrm{II}u}^{(m)} + e^{i\gamma_{\mathrm{II}u}^{(n)}(z_n+D_n)+i\gamma_{\mathrm{I}u}^{(m)}(-z_m'-D_{m-1})}B_1^{(2,1)}\mathbf{e}_{\mathrm{II}u}^{(n)}\mathbf{u}_{\mathrm{I}u}^{(m)} \\
&+e^{i\gamma_{\mathrm{II}u}^{(n)}(z_n+D_n)+i\gamma_{\mathrm{II}u}^{(m)}(-z_m'-D_{m-1})}B_1^{(2,2)}\mathbf{e}_{\mathrm{II}u}^{(n)}\mathbf{u}_{\mathrm{II}u}^{(m)} + e^{i\gamma_{\mathrm{I}u}^{(n)}(z_n+D_n)+i\gamma_{\mathrm{I}d}^{(m)}(-z_m'-D_m)}B_2^{(1,1)}\mathbf{e}_{\mathrm{I}u}^{(n)}\mathbf{u}_{\mathrm{I}d}^{(m)} \\
&+e^{i\gamma_{\mathrm{I}u}^{(n)}(z_n+D_n)+i\gamma_{\mathrm{II}d}^{(m)}(-z_m'-D_m)}B_2^{(1,2)}\mathbf{e}_{\mathrm{I}u}^{(n)}\mathbf{u}_{\mathrm{II}d}^{(m)} + e^{i\gamma_{\mathrm{II}u}^{(n)}(z_n+D_n)+i\gamma_{\mathrm{I}d}^{(m)}(-z_m'-D_m)}B_2^{(2,1)}\mathbf{e}_{\mathrm{II}u}^{(n)}\mathbf{u}_{\mathrm{I}d}^{(m)} \\
&+e^{i\gamma_{\mathrm{II}u}^{(n)}(z_n+D_n)+i\gamma_{\mathrm{II}d}^{(m)}(-z_m'-D_m)}B_2^{(2,2)}\mathbf{e}_{\mathrm{II}u}^{(n)}\mathbf{u}_{\mathrm{II}d}^{(m)} + e^{i\gamma_{\mathrm{I}d}^{(n)}(z_n+D_{n+1})+i\gamma_{\mathrm{I}u}^{(m)}(-z_m'-D_{m-1})}B_3^{(1,1)}\mathbf{e}_{\mathrm{I}d}^{(n)}\mathbf{u}_{\mathrm{I}u}^{(m)} \\
&+e^{i\gamma_{\mathrm{I}d}^{(n)}(z_n+D_{n+1})+i\gamma_{\mathrm{II}u}^{(m)}(-z_m'-D_{m-1})}B_3^{(1,2)}\mathbf{e}_{\mathrm{I}d}^{(n)}\mathbf{u}_{\mathrm{II}u}^{(m)} + e^{i\gamma_{\mathrm{II}d}^{(n)}(z_n+D_{n+1})+i\gamma_{\mathrm{I}u}^{(m)}(-z_m'-D_{m-1})}B_3^{(2,1)}\mathbf{e}_{\mathrm{II}d}^{(n)}\mathbf{u}_{\mathrm{I}u}^{(m)} \\
&+e^{i\gamma_{\mathrm{II}d}^{(n)}(z_n+D_{n+1})+i\gamma_{\mathrm{II}u}^{(m)}(-z_m'-D_{m-1})}B_3^{(2,2)}\mathbf{e}_{\mathrm{II}d}^{(n)}\mathbf{u}_{\mathrm{II}u}^{(m)} + e^{i\gamma_{\mathrm{I}d}^{(n)}(z_n+D_{n+1})+i\gamma_{\mathrm{I}d}^{(m)}(-z_m'-D_m)}B_4^{(1,1)}\mathbf{e}_{\mathrm{I}d}^{(n)}\mathbf{u}_{\mathrm{I}d}^{(m)} \\
&+e^{i\gamma_{\mathrm{I}d}^{(n)}(z_n+D_{n+1})+i\gamma_{\mathrm{II}d}^{(m)}(-z_m'-D_m)}B_4^{(1,2)}\mathbf{e}_{\mathrm{I}d}^{(n)}\mathbf{u}_{\mathrm{II}d}^{(m)} + e^{i\gamma_{\mathrm{II}d}^{(n)}(z_n+D_{n+1})+i\gamma_{\mathrm{I}d}^{(m)}(-z_m'-D_m)}B_4^{(2,1)}\mathbf{e}_{\mathrm{II}d}^{(n)}\mathbf{u}_{\mathrm{I}d}^{(m)} \\
&+e^{i\gamma_{\mathrm{II}d}^{(n)}(z_n+D_{n+1})+i\gamma_{\mathrm{II}d}^{(m)}(-z_m'-D_m)}B_4^{(2,2)}\mathbf{e}_{\mathrm{II}d}^{(n)}\mathbf{u}_{\mathrm{II}d}^{(m)}\Big]
\end{aligned}\tag{8}$$

where

$$\mathbf{B}_1 = \mathbf{Y}_{mn}^{(u)} \cdot \mathbf{M}_m \tag{9}$$

$$\mathbf{B}_2 = \mathbf{B}_1 \cdot \mathbf{G}_u^{(m)}(z_m = -D_{m-1} + D_m) \cdot \mathbf{R}_{Dm,m+1} \tag{10}$$

$$\mathbf{B}_3 = \mathbf{R}_{Un,n-1} \cdot \mathbf{G}_u^{(n)}(z_n = -D_{n-1} + D_n) \cdot \mathbf{B}_1 \tag{11}$$

$$\mathbf{B}_4 = \mathbf{B}_3 \cdot \mathbf{G}_u^{(m)}(z_m = -D_{m-1} + D_m) \cdot \mathbf{R}_{Dm,m+1} \tag{12}$$

When $m < n$,

$$\begin{aligned}
\overline{\overline{G}}_{nm}(\mathbf{r},\mathbf{r}') = -\frac{\omega\mu_m}{4\pi}\int_0^\infty dk_\rho\, k_\rho \cdot J_0(k_\rho\rho)\cdot\Big[& e^{i\gamma_{\mathrm{I}u}^{(n)}(z_n+D_n)+i\gamma_{\mathrm{I}u}^{(m)}(-z'_m-D_{m-1})} C_1^{(1,1)} \mathbf{e}_{\mathrm{I}u}^{(n)} \mathbf{u}_{\mathrm{I}u}^{(m)} \\
&+e^{i\gamma_{\mathrm{I}u}^{(n)}(z_n+D_n)+i\gamma_{\mathrm{II}u}^{(m)}(-z'_m-D_{m-1})} C_1^{(1,2)} \mathbf{e}_{\mathrm{I}u}^{(n)} \mathbf{u}_{\mathrm{II}u}^{(m)} + e^{i\gamma_{\mathrm{II}u}^{(n)}(z_n+D_n)+i\gamma_{\mathrm{I}u}^{(m)}(-z'_m-D_{m-1})} C_1^{(2,1)} \mathbf{e}_{\mathrm{II}u}^{(n)} \mathbf{u}_{\mathrm{I}u}^{(m)} \\
&+e^{i\gamma_{\mathrm{II}u}^{(n)}(z_n+D_n)+i\gamma_{\mathrm{II}u}^{(m)}(-z'_m-D_{m-1})} C_1^{(2,2)} \mathbf{e}_{\mathrm{II}u}^{(n)} \mathbf{u}_{\mathrm{II}u}^{(m)} + e^{i\gamma_{\mathrm{I}u}^{(n)}(z_n+D_n)+i\gamma_{\mathrm{I}d}^{(m)}(-z'_m-D_m)} C_2^{(1,1)} \mathbf{e}_{\mathrm{I}u}^{(n)} \mathbf{u}_{\mathrm{I}d}^{(m)} \\
&+e^{i\gamma_{\mathrm{I}u}^{(n)}(z_n+D_n)+i\gamma_{\mathrm{II}d}^{(m)}(-z'_m-D_m)} C_2^{(1,2)} \mathbf{e}_{\mathrm{I}u}^{(n)} \mathbf{u}_{\mathrm{II}d}^{(m)} + e^{i\gamma_{\mathrm{II}u}^{(n)}(z_n+D_n)+i\gamma_{\mathrm{I}d}^{(m)}(-z'_m-D_m)} C_2^{(2,1)} \mathbf{e}_{\mathrm{II}u}^{(n)} \mathbf{u}_{\mathrm{I}d}^{(m)} \\
&+e^{i\gamma_{\mathrm{II}u}^{(n)}(z_n+D_n)+i\gamma_{\mathrm{II}d}^{(m)}(-z'_m-D_m)} C_2^{(2,2)} \mathbf{e}_{\mathrm{II}u}^{(n)} \mathbf{u}_{\mathrm{II}d}^{(m)} + e^{i\gamma_{\mathrm{I}d}^{(n)}(z_n+D_{n-1})+i\gamma_{\mathrm{I}u}^{(m)}(-z'_m-D_{m-1})} C_3^{(1,1)} \mathbf{e}_{\mathrm{I}d}^{(n)} \mathbf{u}_{\mathrm{I}u}^{(m)} \\
&+e^{i\gamma_{\mathrm{I}d}^{(n)}(z_n+D_{n-1})+i\gamma_{\mathrm{II}u}^{(m)}(-z'_m-D_{m-1})} C_3^{(1,2)} \mathbf{e}_{\mathrm{I}d}^{(n)} \mathbf{u}_{\mathrm{II}u}^{(m)} + e^{i\gamma_{\mathrm{II}d}^{(n)}(z_n+D_{n-1})+i\gamma_{\mathrm{I}u}^{(m)}(-z'_m-D_{m-1})} C_3^{(2,1)} \mathbf{e}_{\mathrm{II}d}^{(n)} \mathbf{u}_{\mathrm{I}u}^{(m)} \\
&+e^{i\gamma_{\mathrm{II}d}^{(n)}(z_n+D_{n-1})+i\gamma_{\mathrm{II}u}^{(m)}(-z'_m-D_{m-1})} C_3^{(2,2)} \mathbf{e}_{\mathrm{II}d}^{(n)} \mathbf{u}_{\mathrm{II}u}^{(m)} + e^{i\gamma_{\mathrm{I}d}^{(n)}(z_n+D_{n-1})+i\gamma_{\mathrm{I}d}^{(m)}(-z'_m-D_m)} C_4^{(1,1)} \mathbf{e}_{\mathrm{I}d}^{(n)} \mathbf{u}_{\mathrm{I}d}^{(m)} \\
&+e^{i\gamma_{\mathrm{I}d}^{(n)}(z_n+D_{n-1})+i\gamma_{\mathrm{II}d}^{(m)}(-z'_m-D_m)} C_4^{(1,2)} \mathbf{e}_{\mathrm{I}d}^{(n)} \mathbf{u}_{\mathrm{II}d}^{(m)} + e^{i\gamma_{\mathrm{II}d}^{(n)}(z_n+D_{n-1})+i\gamma_{\mathrm{I}d}^{(m)}(-z'_m-D_m)} C_4^{(2,1)} \mathbf{e}_{\mathrm{II}d}^{(n)} \mathbf{u}_{\mathrm{I}d}^{(m)} \\
&+e^{i\gamma_{\mathrm{II}d}^{(n)}(z_n+D_{n-1})+i\gamma_{\mathrm{II}d}^{(m)}(-z'_m-D_m)} C_4^{(2,2)} \mathbf{e}_{\mathrm{II}d}^{(n)} \mathbf{u}_{\mathrm{II}d}^{(m)}\Big]
\end{aligned} \tag{13}$$

where

$$\mathbf{C}_4 = \mathbf{Y}_{mn}^{(d)} \cdot \mathbf{N}_m \tag{14}$$

$$\mathbf{C}_3 = \mathbf{C}_4 \cdot \mathbf{G}_d^{(m)}(z_m = -D_m + D_{m-1}) \cdot \mathbf{R}_{Dm,m-1} \tag{15}$$

$$\mathbf{C}_2 = \mathbf{R}_{Dn,n+1} \cdot \mathbf{G}_d^{(n)}(z_n = -D_n + D_{n-1}) \cdot \mathbf{C}_4 \tag{16}$$

$$\mathbf{C}_1 = \mathbf{C}_2 \cdot \mathbf{G}_d^{(m)}(z_m = -D_m + D_{m-1}) \cdot \mathbf{R}_{Um,m-1} \tag{17}$$

It is illustrated that the dyadic Green's functions in the spatial domain are expressed in terms of Sommerfeld integrals in the spectral domain. Among those acceleration techniques for the calculation of the spatial-domain Green's functions, DCIM has been proven to have excellent accuracy and efficiency [10, 11]. In this work, the two-level DCIM is employed to calculate the closed-form Green's functions.

3. NUMERICAL EXAMPLES

This section is to investigate the accuracy and efficiency of the proposed algorithm. Firstly, one element of the field Green's function in the spectral domain is compared with the corresponding portion from the potential Green's function which has been well-documented [9], in the case of the isotropic medium. The relationship between the Green's function in the electric field integral equation (EFIE) and that in the mixed-potential integral equation (MPIE) is as follows,

$$\overline{\overline{G}}^{EJ} = i\omega\mu_0\overline{\overline{G}}^{AJ} + \frac{1}{i\omega\varepsilon_0}\nabla\nabla' G^{VJ} \tag{18}$$

where, $\overline{\overline{G}}^{AJ}$ represents the dyadic Green's functions for magnetic vector potential and G^{VJ} represents the Green's function for electric scalar potential. Fig. 2 shows that the magnitude of $\widetilde{G}_{zz}^{EJ}$ obtained by the present algorithm agrees very well with that from the MPIE.

Secondly, the algorithm is applied to the approximation of the closed-form Green's functions for a four-layer planar uniaxial anisotropic medium. The reference solution, used for the assessment of the accuracy of the closed-form approximation, is obtained through the numerical integration of the spectrum on deformed paths parallel to the real axis [8]. The number of samples is $N = 1024$ for the

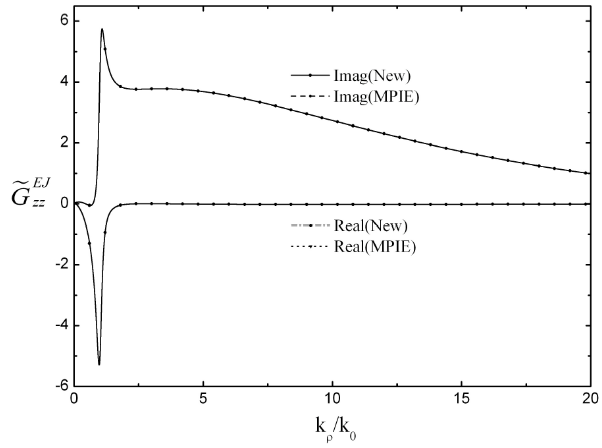

Figure 2: Magnitude of $\widetilde{G}_{zz}^{EJ}$ versus k_ρ for a four-layer isotropic medium. The solid lines correspond to results obtained by the present algorithm while the dots correspond to results from MPIE.

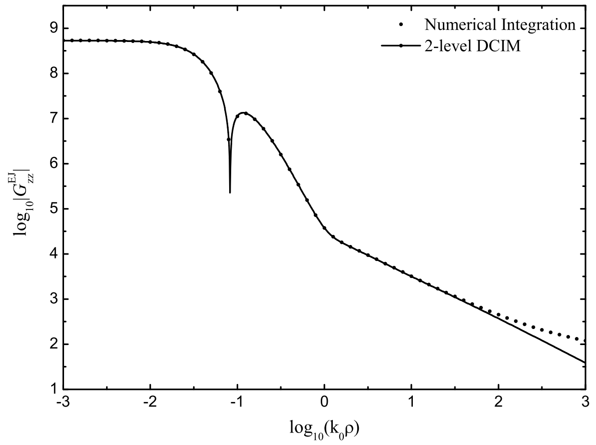

Figure 3: Values of G_{zz}^{EJ} versus ρ for $m = n$. The solid lines correspond to results obtained by the DCIM method while the dots correspond to results obtained by the numerical integration.

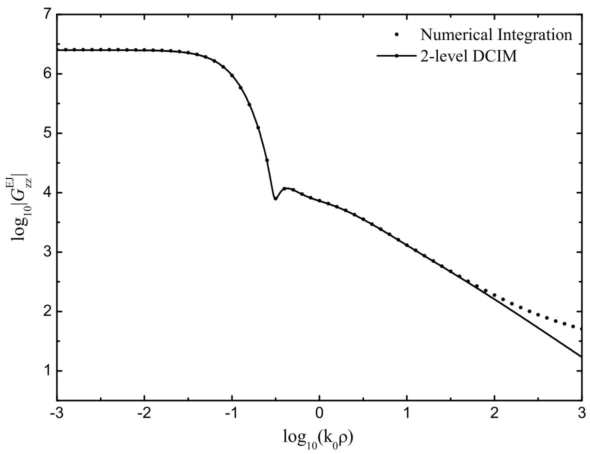

Figure 4: Values of G_{zz}^{EJ} versus ρ for $m < n$. The solid lines correspond to results obtained by the DCIM method while the dots correspond to results obtained by the numerical integration.

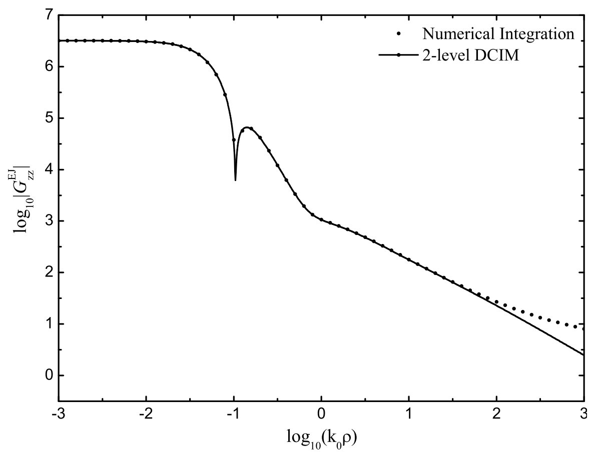

Figure 5: Values of G_{zz}^{EJ} versus ρ for $m > n$. The solid lines correspond to results obtained by the DCIM method while the dots correspond to results obtained by the numerical integration.

path of each level and the operating frequency is 3 GHz. Fig. 3 shows the magnitude of the spatial-domain Green's fucntion G_{zz}^{EJ} evaluated in the case of the source point and the observation point in the same layer (where $m = n = 2$, $z' = -1.2$ mm and $z = -0.2$ mm). The permittivity tensors for the four layers are $\bar{\bar{\varepsilon}}_1 = \varepsilon_0\bar{\bar{I}}$, $\bar{\bar{\varepsilon}}_2 = \{2.1, 0, 0; 0, 2.1, 0; 0, 0, 2.121\}\cdot\varepsilon_0$, $\bar{\bar{\varepsilon}}_3 = \{9.8, 0, 0; 0, 9.8, 0; 0, 0, 9.898\}\cdot\varepsilon_0$ and $\bar{\bar{\varepsilon}}_4 = \varepsilon_0\bar{\bar{I}}$. Fig. 4, shows the magnitude of G_{zz}^{EJ} in the case of $m = 1$, $n = 3$, $z' = 0$ mm and $z = -1.5$ mm. The permittivity tensors are $\bar{\bar{\varepsilon}}_1 = \varepsilon_0\bar{\bar{I}}$, $\bar{\bar{\varepsilon}}_2 = \{2.1, 0, 0; 0, 2.1, 0; 0, 0, 2.31\}\cdot\varepsilon_0$, $\bar{\bar{\varepsilon}}_3 = \{9.8, 0, 0; 0, 9.8, 0; 0, 0, 10.78\}\cdot\varepsilon_0$ and $\bar{\bar{\varepsilon}}_4 = \varepsilon_0\bar{\bar{I}}$. For the magnitude of G_{zz}^{EJ} in Fig. 5, the permittivity tensors are $\bar{\bar{\varepsilon}}_1 = \varepsilon_0\bar{\bar{I}}$, $\bar{\bar{\varepsilon}}_2 = \{2.1, 0, 0; 0, 2.1, 0; 0, 0, 4.2\}\cdot\varepsilon_0$, $\bar{\bar{\varepsilon}}_3 = \{9.8, 0, 0; 0, 9.8, 0; 0, 0, 19.6\}\cdot\varepsilon_0$ and $\bar{\bar{\varepsilon}}_4 = \varepsilon_0\bar{\bar{I}}$. The source point, $z' = -2.5$ mm, is in the layer $m = 3$ and the observation point $z = -0.2$ mm is in the layer $n = 2$. It is demonstrated that the DCIM-based results have an excellent agreement with the numerical integration results in the three cases for $\rho < 15.9\lambda_0$. Here, ρ represents the horizontal distance between the source point and observation point and λ_0 represents the wavelength in the free space. The accuracy could be improved with the extraction of singularity's contribution when $\rho \geq 15.9\lambda_0$. The computational time used for DCIM is less than 60 s for each case, while the computational time for numerical integration method is 137 s per point. It can be inferred from the numerical results that the closed-form Green's function for the stratified uniaxial anisotropic medium can be calculated accurately and efficiently by the present algorithm, compared with the numerical integration results.

4. CONCLUSION

In this paper, a complete set of closed-form Green's functions are provided for the stratified uniaxial anisotropic medium with an arbitrary distribution of electric current sources. The spectral-domain Green's functions in the electric field form are derived by using the wave iterative algorithm. The magnitude of the spectral-domain Green's function based on this algorithm is compared with that obtained from the potential Green's function in isotropic medium and a good agreement is observed. The closed-form Green's functions are calculated by using the 2-level DCIM. Finally, numerical results demonstrate the accuracy and efficiency of the algorithm.

REFERENCES

1. Michalski, K. A. and D. Zheng, "Electromagnetic scattering and radiation by surfaces of arbitrary shape in layered media: Part II: Implementation and results for contiguous half-spaces," *IEEE Trans. Antennas Propagat.*, Vol. 38, No. 3, 345–352, 1990.
2. Geng, N. and L. Carin, "Wide-band electromagnetic scattering from a dielectric BOR buried in a layered lossy dispersive medium," *IEEE Trans. Antennas Propagat.*, Vol. 47, No. 4, 610–619, 1999.
3. Mosig, J. R., "Arbitrarily shaped microstrip structures and their analysis with a mixed potential integral equation," *IEEE Trans. Microw. Theory Tech.*, Vol. 36, No. 2, 314–323, 1988.
4. Park, I., R. Mittra, and M. I. Aksun, "Numerical efficient analysis of planar microstrip configurations using closed-form Green's functions," *IEEE Trans. Microw. Theory Tech.*, Vol. 43, No. 2, 390–400, 1995.
5. Habashy, T. M., S. M. Ali, and J. A. Kong, "Dyadic Green's functions in a planar stratified, arbitrarily magnetized linear plasma," *Radio Science*, Vol. 26, No. 3, 701–715, 1991.
6. Li, L. W., J. H. Koh, T. S. Yeo, M. S. Leong, and P. S. Kooi, "Cylindrical vector eigenfunciton expansion of green dyadics for multilayered anisotropic media and its application to four-layered forest," *IEEE Trans. Antennas Propagat.*, Vol. 52, No. 2, 466–477, 2004.
7. Aksun, M. I., "A robust approach for the derivation of closed-form Green's functions," *IEEE Trans. Microwave Theory Tech.*, Vol. 44, No. 5, 651–658, 1996.
8. Chew, W. C., *Waves and Fields in Inhomogeneous Media*, Van Nostrand Reinhold, New York, 1990.
9. Zhang, M., L. W. Li, and Y. F. Tian, "An efficient approach for extracting poles of Green's functions in general multilayered media," *IEEE Trans. Antennas Propagat.*, Vol. 56, No. 1, 269–273, 2008.